EXAMINING THE EFFECT OF THE NEW CHEMICAL COMPOSITION ON SOLAR STRUCTURE BY USING THE ADIABATIC INDEX

Chia-Hsien Lin[1], H. M. Antia[2], and Sarbani Basu[1]

[1]*Astronomy Department, Yale University, New Haven CT06511, U.S.A.*
[2]*Tata Institute of Fundamental Research, Homi Bhabha Road, Mumbai 400005, India*

ABSTRACT

Recently, Asplund et al. (2004) and Asplund et al. (2005) (AGS hereafter), using a refined model for the solar atmosphere, announced the new solar chemical composition with the heavy-element abundance ($Z = 0.0122$) being about 30% lower than the previously determined value ($Z = 0.0171$; Grevesse & Sauval (1998); GS98 hereafter). In this study, we use the adiabatic index, $\Gamma_1 \equiv (\partial \ln P/\partial \ln \rho)_s$, to examine and isolate the effects of different chemical compositions. Specifically, we exploited the fact that Γ_1 deviates from the isentropic value of $5/3$ in the element ionization zones, which are determined by the equation-of-state (EOS) formalism and the element abundance and are independent of the macrophysical properties (e.g., P, ρ). The results of our study can provide an independent test of the newly determined solar composition.

Key words: Sun:interior,Sun:oscillations,Sun:abundances.

1. OBJECTIVES

We have two aims: First is to use the discrepancy in Γ_1 between the Sun and the models with different Z/X (X is hydrogen abundance) to try to infer the possible Z/X in the solar convective zone, and second is to investigate the effects of varying the abundance of individual element and the possible cancellation/compensation effects between different elements.

2. THE INVERSION TECHNIQUE

The inversion method is based on a linear relation between the relative frequency difference $\delta\omega/\omega$ and relative difference in structure (e.g., Γ_1 in this study). In practice, the inversion compares Γ_1 at the same *depth*. Such $\delta\Gamma_1/\Gamma_1$ is a result of the discrepancies in both macrophysical structure (e.g., P, ρ) and microphysical properties (e.g., EOS, chemical composition) at that depth. To extract $\delta\Gamma_1/\Gamma_1$ that reflects only microphysical discrepancies, we followed the technique proposed by Basu & Christensen-Dalsgaard (1997):

$$\frac{\delta\Gamma_1}{\Gamma_1} = \left(\frac{\partial \ln \Gamma_1}{\partial \ln P}\right)_{Y,\rho} \frac{\delta P}{P} + \left(\frac{\partial \ln \Gamma_1}{\partial \ln \rho}\right)_{Y,P} \frac{\delta \rho}{\rho} + \left(\frac{\partial \ln \Gamma_1}{\partial Y}\right)_{P,\rho} \delta Y + \frac{\delta\Gamma_{1,\rm int}}{\Gamma_{1,\rm int}}, \quad (1)$$

where Y is the Helium abundance, and $\delta\Gamma_{1,\rm int}/\Gamma_{1,\rm int}$ is the relative difference caused by the microphysical discrepancies, and is called "intrinsic" Γ_1 difference. Consequently, the linear relation between $\delta\omega/\omega$ and $\delta\Gamma_{1,\rm int}/\Gamma_{1,\rm int}$ is as follows:

$$\frac{\delta\omega_i}{\omega_i} = \int_0^R K^i_{u,Y}(r)\frac{\delta u}{u}(r)dr + \int_0^R K^i_{Y,u}(r)\delta Y(r)dr + \int_0^R K^i_{c^2,\rho}(r)\frac{\delta\Gamma_{1,\rm int}}{\Gamma_{1,\rm int}}(r)dr + \frac{F_{\rm surf}(\omega_i)}{Q_i}, \quad (2)$$

where, K^i are kernels, $u \equiv P/\rho$ is the isothermal sound speed, c is the adiabatic sound speed, and $F_{\rm surf}(\omega_i)/Q_i$ represents the effect of uncertainties in the model close to the surface, and is usually called the "surface term". Q_i is a measure of the mode inertia.

The structural difference (e.g., $\delta\Gamma_{1,\rm int}/\Gamma_{1,\rm int}$) is revealed by inverting the above equation to obtain a localized average of $\delta\Gamma_{1,\rm int}/\Gamma_{1,\rm int}$. That is,

$$\left\langle \frac{\delta\Gamma_{1,\rm int}}{\Gamma_{1,\rm int}} \right\rangle \approx \sum_i a_i \frac{\delta\omega_i}{\omega_i},$$

where $\{a_i\}$ is a set of weighting parameters.

3. THE MODELS AND THE OBSERVATIONAL DATA

We use a variety of models for this work. They are listed in Table 1. The models have been constructed with CEFF EOS (Eggleton et al., 1973; Guenther et al., 1992; Christensen-Dalsgaard & Däppen, 1992) because

Table 1

Model Name	Z/X	Mixture	Enhancements
Z245	0.0245	GS98	
Z230	0.0230	GS98	
Z165	0.0165	GS98	
AGS165	0.0165	AGS	
AGS209	0.0209	AGS	
AGS209Ne2	0.0209	AGS*	Ne= 2×Ne of AGS
AGS209Ne4	0.0209	AGS*	Ne= 4×Ne of AGS
AGS197Ne2CNO	0.0209	AGS*	Ne= 2×Ne of AGS
			C,N,O enhanced by 1σ of C,N,O of AGS
C2	0.0245	GS98*	C= 2×C of GS
O2	0.0245	GS98*	O= 2×O of GS
Ne2	0.0245	GS98*	Ne = 2×Ne of GS
C1.5	0.0245	GS98*	C= 1.5×C of GS
O1.5	0.0245	GS98*	O= 1.5×O of GS
Ne1.5	0.0245	GS98*	Ne= 1.5×Ne of GS
C2O1.5	0.0245	GS98*	C= 2×C of GS
			O= 1.5× O of GS
C1.5O1.5	0.0245	GS98*	C= 1.5× C of GS
			O= 1.5× O of GS
C0.5O1.5	0.0245	GS98*	C= 0.5× C of GS
			O= 1.5× O of GS
C1.5O1.5Ne1.5	0.0245	GS98*	C = 1.5 × C of GS
			O= 1.5× O of GS
			Ne= 1.5×O of GS

GS98: mixture determined by Grevesse & Sauval (1998)
GS98*: GS98 with enhancements of certain elements as noted in Special characteristics
AGS: mixture determined by Asplund et al. (2005)
AGS*: AGS with enhancements of certain elements as noted in Special characteristics

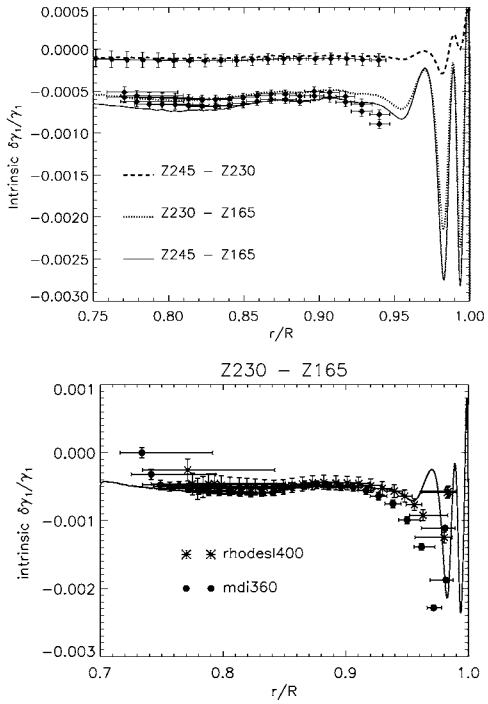

Figure 1. The upper panel is to illustrate the effect of different Z/X on $\delta\Gamma_{1,\rm int}/\Gamma_{1,\rm int}$. The lower panel is a comparison of the inversion results using two mode sets, mdi360, which contains modes up to $l = 190$, and rhodesl400, which contains modes up to $l = 400$ from rhodes1998 mode set. In both panels, The solid lines are the computed $\delta\Gamma_{1,\rm int}/\Gamma_{1,\rm int}$ between models with different Z/X as denoted in the figure. The inverted values are overplotted as symbols along with error bars. The upper panel shows that the discrepancy in Z/X can be identified as a parallel shift by our inversion. The lower panel shows that using high-degree modes improves the inversion accuracy near the surface.

the abundance ratios can be tuned in CEFF but not in other EOS, such as OPAL and MHD.

The helioseismic data used in this study were obtained by the Michelson Doppler Imager (MDI) (Schou et al., 1998). The dataset contains f-modes up to $l = 250$ and p-modes up to $l = 190$.

For the inversions between models, we selected only the modes that are also present in the observational data. The observational errors are assigned to these selected model frequencies. The data sets used for our mode selection are the aforementioned MDI 360-day observation, which we call mdi360, and the high-degree mode set from Rhodes et al. (1998), which is based on 61 days of data collected by the SOI/MDI instrument beginning in May 1996. We refer to this set as rhodes1998. This data set contains f-modes and p-modes up to $l = 1000$.

4. RESULTS

4.1. Signatures of difference in Z/X and the inferred solar Z/X

Figure 1 shows that the difference in Z/X causes large and sharp features in $\delta\Gamma_{1,\rm int}/\Gamma_{1,\rm int}$ near the surface ($r/R_\odot > 0.92$, $R_\odot$ is the solar radius). In the deeper region, the difference in Z/X mainly results in a parallel shift. The lower panel of the figure shows that the inversion accuracy near the surface can be improved by simply including p modes up to $l = 400$. However, even with only p modes up to $l = 190$ (i.e., mdi360 mode set) the discrepancy in Z/X can be identified as a parallel shift in deeper layers.

The upper panel of Fig. 2 shows that the separation between Sun–Z245 and Sun–Z230 are of 1σ level and the separation between Sun–Z165 and Sun–AGS165 are

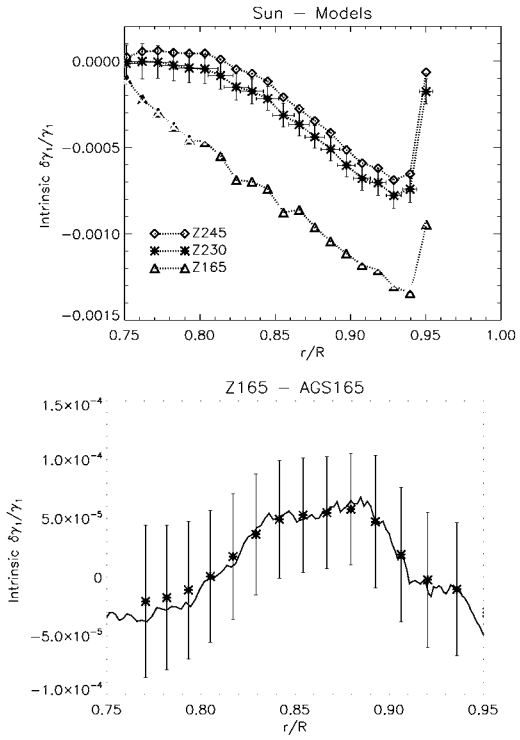

Figure 2. The inversion results between the Sun and models are plotted in the upper panel. Only one set of the errors are plotted for the sake of clarity. The lines connecting the symbols are added to guide the eyes. The lower panel shows the computed (line) and inverted (stars) $\delta\Gamma_{1,\rm int}/\Gamma_{1,\rm int}$ of Z165–AGS165, which reflects the abundance-ratio difference between GS98 and of AGS. The plots show that the reduction in Z/X from GS98 (0.0230) to AGS (0.0165) has greater effects than the difference in the abundance ratio between the two compositions.

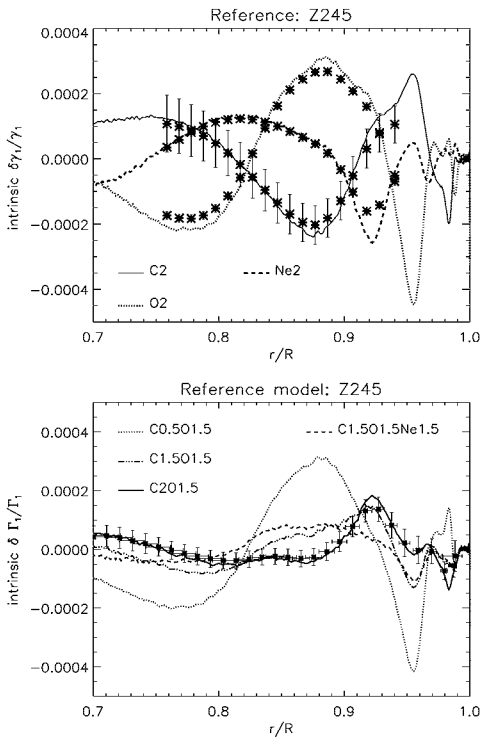

Figure 3. The upper panel shows the effects of individually enhancing C, O, and Ne. The possibility of cancelling opposite features (i.e., producing $\delta\Gamma_{1,\rm int}/\Gamma_{1,\rm int} \approx 0$ between two models with different compositions) is examined and illustrated in the lower panel. The computed $\delta\Gamma_{1,\rm int}/\Gamma_{1,\rm int}$ in both panels are plotted as lines. The symbols and the error bars are the inverted values to show the accuracy of our inversion. The lower panel shows that the residual features after the attempted cancellation are greater than the inversion errors, and can be identified by our inversion.

smaller than the error bars. The lower panel is to explicitly show that $\delta\Gamma_{1,\rm int}/\Gamma_{1,\rm int}$ of Z165–AGS165 is smaller than the current inversion errors. In other words, inversions with current mode set can barely distinguish Z245 and Z230, and cannot distinguish Z165 and AGS165.

The results clearly favour the previous heavy element abundance (i.e., $Z/X = 0.0245$ and 0.0230) over the latest, lower value, $Z/X = 0.0165$. However, we need to keep in mind that $\delta\Gamma_{1,\rm int}/\Gamma_{1,\rm int}$ reflects the discrepancies in both the EOS and the chemical composition. Hence, with no other EOS with same chemical compositions to compare with, we can only conclude from the figure that $Z/X = 0.0230$ and 0.0245 is better than $Z/X = 0.0165$ for a model implemented with the CEFF EOS. This is consistent with the results by Basu & Antia (in these proceedings).

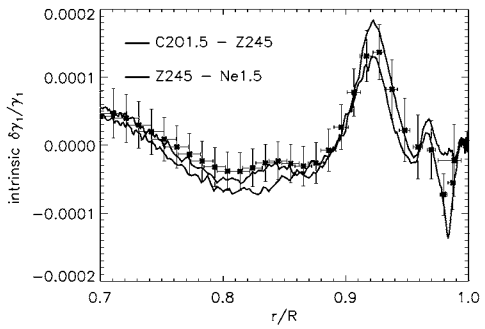

Figure 4. Similar $\delta\Gamma_{1,\rm int}/\Gamma_{1,\rm int}$ resulting from different chemical compositions. The solid lines are the computed values, and the symbols and error bars are the inverted values. This example shows that reducing Ne abundance and enhancing C, O abundances produce similar $\delta\Gamma_{1,\rm int}/\Gamma_{1,\rm int}$. The difference between the two curves is comparable to our inversion errors.

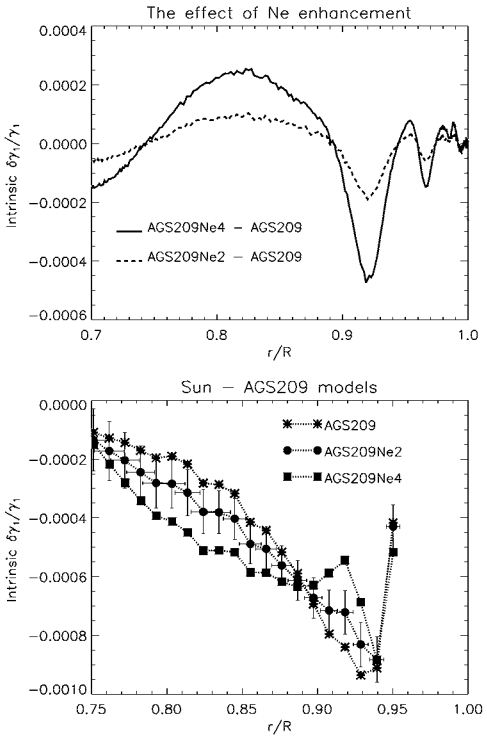

Figure 5. The effect of enhancing Ne in the AGS mixture. The computed $\delta\Gamma_{1,\rm int}/\Gamma_{1,\rm int}$ of AGS209Ne4–AGS209 and AGS209Ne2–AGS209 are plotted in the upper panel. The curves show that Ne enhancement reduces Γ_1 at $r \approx 0.92R_\odot$ and increases Γ_1 in the deeper region. The lower panel shows the inverted $\delta\Gamma_{1,\rm int}/\Gamma_{1,\rm int}$ between the Sun and these three AGS209 models. Only one set of error bars are plotted for the sake of clarity.

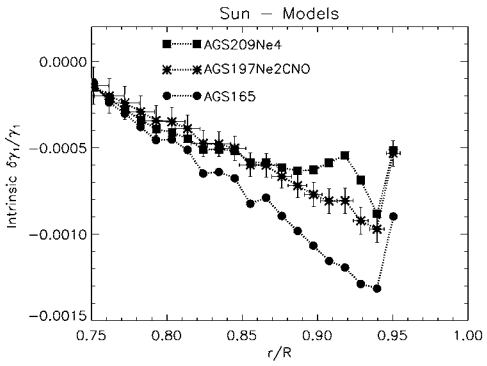

Figure 6. The inverted $\delta\Gamma_{1,\rm int}/\Gamma_{1,\rm int}$ between the Sun and AGS165, AGS209Ne4, and AGS197Ne2CNO. Only one set of the errors are plotted for the sake of clarity. The dotted lines are added to guide the eyes. The comparison of the three curves indicates that enhancing the abundance of individual element improves the models in the region $r > 0.83R_\odot$. However, this is still insufficient to bring the models into complete seismic agreement with the Sun.

4.2. Signatures of the difference in element abundances

The effects of enhancing individual elements and the possibility of eliminating $\delta\Gamma_{1,\rm int}/\Gamma_{1,\rm int}$ between two models with different chemical compositions are illustrated in Fig. 3. The inverted results were overplotted to show the accuracy of the inversion. In the lower panel, the abundances in the test models were tuned to eliminate the features seen in the upper panel. The figure shows that the differences are unlikely to be completely cancelled. The residual features after the attempted cancellation are above the error level of our inversion.

Fig. 4 demonstrates that the effect of reducing Ne abundance can be reproduced by enhancing C and O with no change to Ne abundance. The difference between the two models is comparable to the inversion errors.

Fig. 5 shows that enhancing Ne in AGS mixture reduces the near-surface discrepancy between the Sun and models. The resulting $\delta\Gamma_{1,\rm int}/\Gamma_{1,\rm int}$ curve is flatter than the curve of Sun–AGS165 (see Fig. 6).

5. SUMMARY AND DISCUSSION

Our inversion for the intrinsic Γ_1 difference, $\delta\Gamma_{1,\rm int}/\Gamma_{1,\rm int}$, can identify the discrepancy in Z/X as a parallel shift and the discrepancy in element abundances as deformation of the function. The inversion with p modes up to $l = 190$ becomes inaccurate near the surface (i.e., $r > 0.9R_\odot$). We show that the inversion accuracy in this near-surface region can be improved by simply including p modes up to $l = 400$. We found that different composition discrepancies may result in similar $\delta\Gamma_{1,\rm int}/\Gamma_{1,\rm int}$ profiles that cannot be distinguished by our inversion (cf. Fig. 4). This may suggest that models with different chemical compositions could have similar $\Gamma_{1,\rm int}$ profiles. In other words, $\delta\Gamma_{1,\rm int}/\Gamma_{1,\rm int}$ could be nearly zero even if the two models have different chemical compositions. However, we did not find such cases. Our attempts, as demonstrated in Fig. 3, show that reducing $\delta\Gamma_{1,\rm int}/\Gamma_{1,\rm int}$ at one location often leads to increasing the difference at other locations. The residual features after the attempted cancellation are above our inversion errors.

Individually enhancing C, O, and Ne shows very discernible $\delta\Gamma_{1,\rm int}/\Gamma_{1,\rm int}$ (Fig. 3 upper panel). However, when both C and O are enhanced (e.g., the difference between models C1.5O1.5 and Z245), the resulting $\delta\Gamma_{1,\rm int}/\Gamma_{1,\rm int}$ is very small (cf. Fig. 3 lower panel). Therefore, it is possible that the similarity between model Z165 (GS98 abundances; $Z/X = 0.0165$) and model AGS165 (AGS abundances; $Z/X = 0.0165$) is because the features from the abundance discrepancies in C and O cancel each other.

The effect of reducing total Z from GS98 ($Z/X = 0.0230$) to AGS ($Z/X = 0.0165$) is significantly greater

than the effect of reducing the abundance ratio from GS98 to AGS. This is also seen by Basu & Antia (in these proceedings). Our inversion results favour the Z/X from GS98 over the new Z/X from AGS. However, since $\delta\Gamma_{1,\rm int}/\Gamma_{1,\rm int}$ reflects the effects from both equation of state and chemical composition, we can only conclude that $Z/X = 0.0230$ and 0.0245 with GS98 composition is best for a model implemented with CEFF EOS.

The large discrepancy at $0.9 < r/R_\odot < 0.95$ commonly seen in all models implemented with CEFF EOS (cf. Fig. 2) could be partly due to the inaccuracy in the EOS. Our results indicate that this discrepancy can be reduced by enhancing Ne (cf. Fig. 6). Such cancellation of discrepancies further emphacises that $\delta\Gamma_{1,\rm int}/\Gamma_{1,\rm int}$ reflects the combined effects from the chemical composition and equation of state.

ACKNOWLEDGMENTS

This work utilizes data from the Solar Oscillations Investigation / Michelson Doppler Imager (SOI/MDI) on the Solar and Heliospheric Observatory (SOHO). SOHO is a project of international cooperation between ESA and NASA. MDI is supported by NASA grant NAG5-8878 to Stanford University.

This work is partially supported by NSF grant ATM 0348837 and NASA grant NNG06D13C to SB.

REFERENCES

Asplund, M., Grevesse, N., & Sauval, A. J. 2005, in ASP Conf. Ser. 336: Cosmic Abundances as Records of Stellar Evolution and Nucleosynthesis, ed. T. G. Barnes & F. N. Bash, 25

Asplund, M., Grevesse, N., Sauval, A. J., Allende Prieto, C., & Kiselman, D. 2004, Astronomy & Astrophysics, 417, 751

Basu, S. & Christensen-Dalsgaard, J. 1997, Astronomy & Astrophysics, 322, L5

Christensen-Dalsgaard, J. & Däppen, W. 1992, Astronomy & Astrophysics Review, 4, 267

Eggleton, P. P., Faulkner, J., & Flannery, B. P. 1973, Astronomy & Astrophysics, 23, 325

Grevesse, N. & Sauval, A. J. 1998, in Solar Composition and Its Evolution – From Core to Corona, ed. C. Fröhlich, M. C. E. Huber, S. K. Solanki, & R. von Steiger, 161

Guenther, D. B., Demarque, P., Kim, Y.-C., & Pinsonneault, M. H. 1992, Astrophysics Journal, 387, 372

Rhodes, Jr., E. J., Reiter, J., Kosovichev, A. G., Schou, J., & Scherrer, P. H. 1998, in Structure and Dynamics of the Interior of the Sun and Sun-like Stars SOHO 6/GONG 98 Workshop Abstract, June 1-4, 1998, Boston, Massachusetts, p. 73, ed. S. Korzennik, 73

Schou, J., Christensen-Dalsgaard, J., Howe, R., et al. 1998, in Structure and Dynamics of the Interior of the Sun and Sun-like Stars SOHO 6/GONG 98 Workshop Abstract, June 1-4, 1998, Boston, Massachusetts, p. 845, ed. S. Korzennik, 845